

Modeling COVID-19 pandemic with financial markets models: The case of Jaén (Spain)

Julio Guerrero*

*Department of Mathematics, University of Jaén,
Campus Las Lagunillas s/n, 23071 Jaén, Spain and
Institute Carlos I of Theoretical and Computational Physics (iC1),
University of Granada, Fuentenueva s/n, 18071 Granada, Spain*

Maria del Carmen Galiano

Department of Mathematics, University of Jaén, Campus Las Lagunillas s/n, 23071 Jaén, Spain

Giuseppe Orlando†

Department of Economics and Finance, University of Bari, Largo Abbazia S. Scolastica, Bari, 70124, Italy

The main objective of this work is to test whether some stochastic models typically used in financial markets could be applied to the COVID-19 pandemic. To this end we have implemented the ARIMAX and Cox-Ingersoll-Ross (CIR) models originally designed for interest rate pricing but transformed by us into a forecasting tool. For the latter, which we denoted CIR*, both the Euler-Maruyama method and the Milstein method were used. Forecasts obtained with the maximum likelihood method have been validated with 95% confidence intervals and with statistical measures of goodness of fit, such as the root mean square error (RMSE). We demonstrate that the accuracy of the obtained results is consistent with the observations and sufficiently accurate to the point that the proposed CIR* framework could be considered a valid alternative to the classical ARIMAX for modelling pandemics.

Keywords: **COVID-19, Forecasting, Cox-Ingersoll-Ross model, ARIMAX, Milstein method**

arXiv:2301.08803v1 [q-bio.PE] 20 Jan 2023

* jguerrer@ujaen.es

† giuseppe.orlando@uniba.it: corresponding author

I. INTRODUCTION

Coronavirus disease 2019 (COVID-19) is a lung disease caused by severe acute respiratory syndrome coronavirus 2 (SARS-CoV-2). In December 2019, the Chinese authorities reported different cases of this virus in Wuhan. This disease spread rapidly throughout the world from less than 30 cases at the end of December 2019 to more than 8,455,738 confirmed cases on June 20, 2021.

The first case in Spain was a German tourist, on January 31, 2021. From that moment, several cases began to be confirmed throughout the country. In Andalusia, the first positive was detected in Seville on February 26, 2020. Two days later the first case was confirmed in the province of Jaén, and on March 6 the first case of coronavirus in the city of Jaén.

As the days went by, after the high number of infections in the country, the state of alarm was decreed on March 14, which was extended until June 21. The application of measures such as the use of a mask, perimeter confinements, the closure of non-essential services, etc., improved the infection rate two weeks after the declaration of quarantine. During these years, many researchers from various disciplines have used various modelling tools to analyze the impact of the pandemic at the global and local levels. In our case, we are going to focus on modelling the contagion in Jaén in two different ways. The first approach is based on the Autoregressive Integrated Moving Average with Explanatory Variable (ARIMAX) model [1] which, we found, provides better performances than the Autoregressive Integrated Moving Average (ARIMA) (on the same line, see also [2–6]). This is a common model in time series forecasting and is often adopted in finance [7–10].

The second approach is based on the Cox, Ingersoll and Ross (CIR) model. This is a model designed for interest rates pricing that we turn into a forecasting tool. We prove that this transformation of the CIR model, which we have denoted CIR*, outperforms the classical ARIMAX. For the latter, both the Euler-Maruyama method and the Milstein method were used and this is the main contribution of the present study. Notice that the suggested approach not only extends the models available to scholars to model pandemics but, also, paves the way for similar approaches where financial models can be converted into econometric models.

For the implementation of real-world data, we use the data from the moving averages for 14 days of the daily cases of city of Jaén, that is, each data represents the average number of people infected in each of the previous 14 days. This is because, due to the weekend effect and occasional misreporting, we found that the moving average is a more reliable target. This is due to two reasons: a) the relatively small size of the city of Jaén, which affects the number of cases and b) the effect of the weekend when reporting is altered. The two effects lead to highly irregular behavior in the time series considered. Over that time series, we estimate the parameters of the considered models, in such a way that they best fit the data. The forecasts have been validated with 95% confidence intervals and with statistical measures of goodness of fit, such as the RMSE.

This article is organized as follows. Section II briefly summarizes the literature. Section III reports the data, describes the CIR model as well as the methodology on which it is based. That is followed by the explanation the suggested adaptation to forecasting, by its calibration and by a sketch of the ARIMAX model. Section IV shows the obtained results of the two models by comparing them. Section V concludes.

II. LITERATURE REVIEW

Among those works that adopted the ARIMA (and the like models) to estimate the cases of the COVID-19 pandemic, we mention Ekinici [11] who considered data from USA, India, Brazil, France, Russia, UK, Italy, Spain and Germany. When comparing ARMA-GARCH, ARMA-TGARCH and ARMA-EGARCH models, it was found that while considering the conditional variance effect improves the forecasting power, the asymmetric effect (such as asymmetric GARCH models) has mixed results. Sahai et al. [12] adopted the ARIMA for analyzing the trend of COVID-19 cases in Spain, Italy, France, Germany and the US. The authors claim that their model provides considerable forecast accuracy and could be a useful tool for governments to ramp up their healthcare preparations. Subramaniam et al. [8] draw a parallel between forecasting stock prices and cases of the pandemic by means of the ARIMA model. Then, they explore the correlation between the predictive efficiency of the ARIMA model and variation in the data. Katoch et al. [13] adopt an ARIMA model to analyse the temporal dynamics of the COVID-19 outbreak in India from 30 January 2020 to 16 September 2020. Their approach suggests "varying epidemic's inflexion point and final size for underlying states and the mainland, India". Regarding the alternative between ARIMA and ARIMAX, in the literature has been found that the latter may yield better forecast compared to the seasonal ARIMA (SARIMA) model and Neural Networks (e.g. see Suhartono [14]). This is because the ARIMAX is most suited to deal with calendar effects [2–5, 15].

As regards the Cox, Ingersoll and Ross (CIR) model [16, 17], as already mentioned, it has been proposed for the pricing of interest rates. At the time of its introduction, it quickly gained popularity in finance because it

was perceived as "an improvement on the Vasicek model [18], not allowing for negative rates and introducing rate-dependent volatility, as well as for its relatively handy implementation and analytical tractability" [19].

Other applications of the CIR model include stochastic volatility modelling in option pricing problems [20, 21] or default intensities in credit risk [22, 23]. In this study, similar to what has been done by Orlando and at. [19, 24–26], when developing the CIR# model, we transform the original CIR model into a forecasting tool and compare its performance with that of the well known ARIMAX model.

III. MATERIALS AND METHODS

A. Data

The available data are the moving averages of 14 days of infections in the city of Jaén, from February 2, 2020 to October 8, 2021 and have been provided by the Health and Family Council of the Andalusian Regional Government (see Figure 1). Jaén is a relatively small city (around 110 thousand inhabitants), which represents a challenge since the number of COVID-19 daily cases is small and with large fluctuations, even after the moving averages are computed. Therefore we shall have the opportunity of testing different methods in unfavourable circumstances.

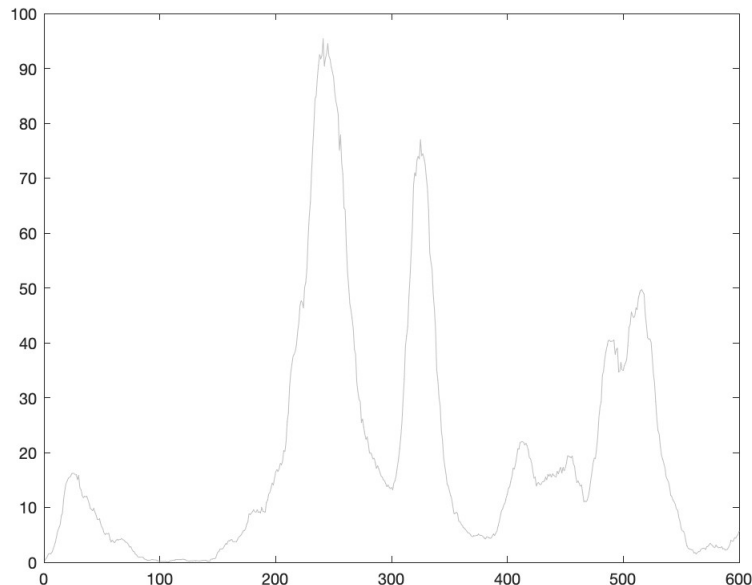


FIG. 1. 14-day moving average of the daily cases of COVID-19 in the city of Jaén. The abscissa represents the days elapsed since February 2, 2021.

B. ARIMAX model

Leaving aside the cases where data show evidence of non-stationarity where an initial differencing removes the integrated (I) part, the ARMAX model can be described as:

$$\begin{aligned}
 y(t) + a_1 y(t-1) + \dots + a_{n_a} y(t-n_a) = & \\
 & b_1 x(t-n_k) + \dots + b_{n_b} x(t-n_k-n_b+1) + \\
 & c_1 \varepsilon(t-1) + \dots + c_{n_c} \varepsilon(t-n_c) + \varepsilon(t)
 \end{aligned} \tag{1}$$

with, $y(t)$ dependent/output variable at time t , n_a , number of poles, n_b number of zeroes plus 1, n_c number of c coefficients, n_k dead time in the system. Moreover, $y(t-1) \dots y(t-n_a)$ denotes the dependence between the current

output and the previous outputs, $x(t - n_k) \dots x(t - n_k - n_b + 1)$ indicates the dependence between the current output and both the previous and delayed inputs, and $\epsilon(t)$ expresses a white-noise error.

The orders of the ARMAX model are given by the parameters n_a, n_b , and n_c whilst n_k is the delay and q is the delay operator. The ARMAX in compact form can be written as

$$A(q)y(t) = B(q)x(t - n_k) + C(q)\epsilon(t) \quad (2)$$

such that,

$$\begin{aligned} A(q) &= 1 + a_1q^{-1} + \dots + a_{n_a}q^{-n_a} \\ B(q) &= b_1 + b_2q^{-1} + \dots + b_{n_b}q^{-n_b+1} \\ C(q) &= 1 + c_1q^{-1} + \dots + c_{n_c}q^{-n_c}. \end{aligned}$$

The ARIMAX model can be seen as a generalization of the ARIMA because adds to the structure above described an integrator in the white noise $\epsilon(t)$ as follows:

$$A(q)y(t) = B(q)x(t - nk) + \frac{C(q)}{(1 - q^{-1})}\epsilon(t). \quad (3)$$

1. Estimation of the ARIMAX model

To estimate the ARIMAX model the following steps have been performed.

1. Ensure stationarity of the times series by conducting Augmented Dicky Fuller (ADF) Test.
2. Model identification, i.e. specification of the autoregressive (AR) and moving average (MA) terms with the help of the autocorrelation function (ACF) and partial autocorrelation function (PACF).
3. Parameter estimation according to Ljung [27] and related implementation in Matlab [28]. The best model is selected based on Akaike information criterion (AIC) values [29].

From now on, we refer to the ARMAX model (and not to the ARIMAX) assuming that the integration (I) has been removed.

C. CIR* model

As mentioned, this model emerged in 1985 from the hand of John C. Cox, Jonathan E. Ingersoll and Stephen A. Ross [16, 17] as an improvement of the Vasicek model to prevent negative interest rates.

The CIR model is based on the following equation:

$$\begin{cases} dX_t = \alpha(\mu - X_t) dt + \sigma\sqrt{X_t}dW_t \\ X_0 = x_0 \end{cases} \quad (4)$$

Here, α, μ and σ are positive constants, $X(t)$ is the interest rate, t is time, and W_t denotes the standard Wiener process.

The parameters include the following:

- $\alpha(\mu - X_t)$ is the same factor as in Vasicek's model, so the interpretation of the deterministic solution is the same.
- The standard deviation factor $\sigma\sqrt{X_t}$ removes negative rates.
- $\sqrt{X_t}$ increases the standard deviation as the short-term rate increases.

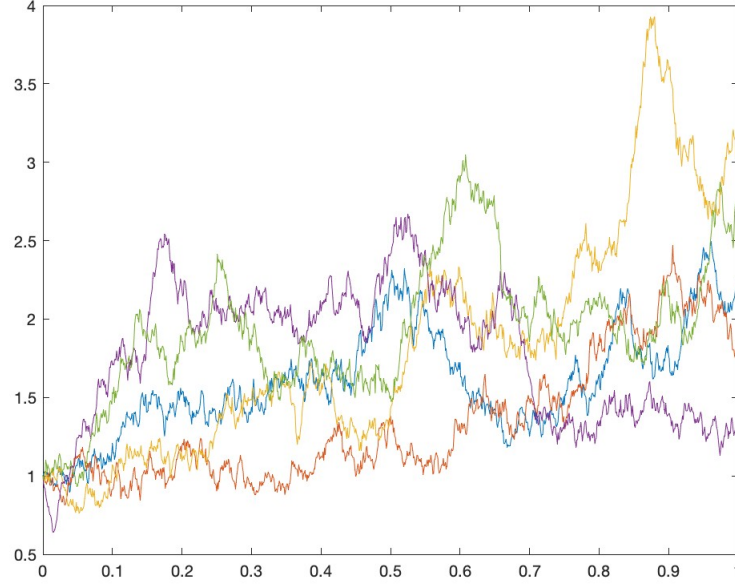


FIG. 2. Simulated paths of the CIR model

This model can only have positive solutions since when the interest rate is 0 it ends up being positive later on. Also, when it is low or close to 0, the standard deviation is close to 0.

The only solution to (4) is what is known as the CIR process. Integrating Eq. (4):

$$X_t = X_s + \alpha \int_s^t (\mu - X_u) du + \sigma \int_s^t \sqrt{X_u} dW_u, \quad s < t \quad (5)$$

therefore

$$E[X_t|X_s] = X_s + \alpha \int_s^t (\mu - E[X_t|X_s]) du, \quad s < t$$

If we call $m_t = E[X_t|X_s]$ we have

$$\frac{d}{dt} m_t = \alpha(\mu - m_t), \quad s < t$$

whose solution is:

$$m_t = X_s e^{-\alpha(t-s)} + \mu(1 - e^{-\alpha(t-s)})$$

So

$$E[X_t|X_s] = X_s e^{-\alpha(t-s)} + \mu(1 - e^{-\alpha(t-s)}), \quad s < t \quad (6)$$

and therefore

$$E[X_t|X_s] - \mu = (X_s - \mu)e^{-\alpha(t-s)}, \quad s < t \quad (7)$$

Thus $E[X_t|X_s] - \mu$ has the same sign as $X_s - \mu$. In addition, if $\mu > 0$ and $\alpha > 0$, starting with $X_s > 0$ we conclude that $X_t > 0$.

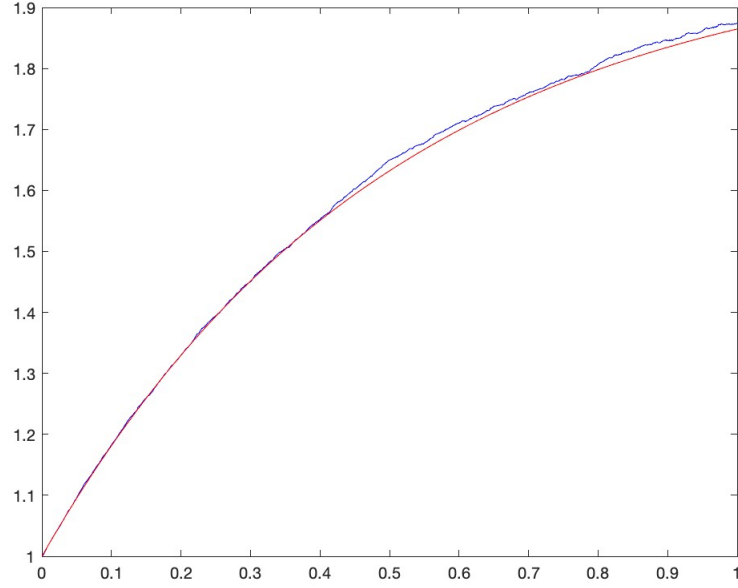


FIG. 3. Numerical (blue) and theoretical (red) mean comparison of the CIR model with Euler's method for 1000 paths, with $x_0 = 1$, $\alpha = 2$, $\mu = 2$ and $\sigma = 1$ and 5000 subintervals.

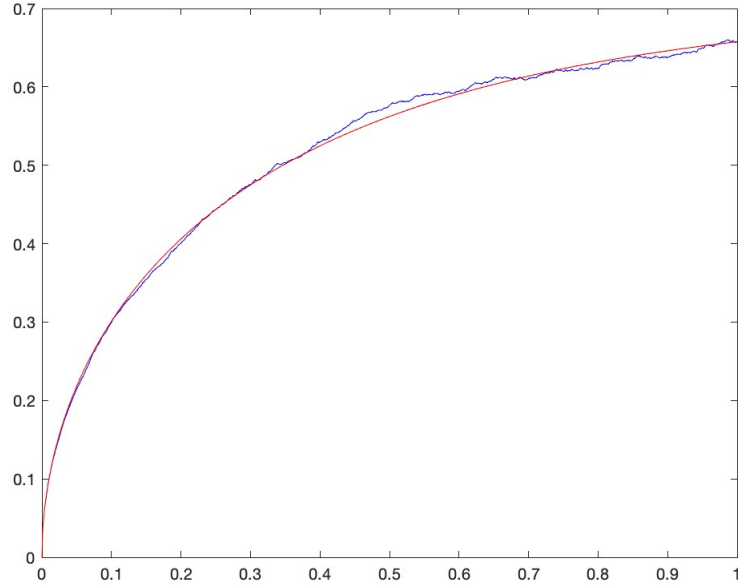


FIG. 4. Comparison of the numerical (blue) and theoretical (red) standard deviation of the CIR model with the Euler method for paths of 1000, with $x_0 = 1$, $\alpha = 2$, $\mu = 2$ and $\sigma = 1$ and 5,000 subintervals

Similarly, the variance is found to be:

$$\text{Var}[X_t|X_s] = \frac{X_s \sigma^2}{\alpha} (e^{-\alpha(t-s)} - e^{-2\alpha(t-s)}) + \frac{\mu \sigma^2}{2\alpha} (1 - e^{-\alpha(t-s)})^2 \quad (8)$$

As stated at the beginning, the fundamental advantage of this model is that the solutions are nonnegative. However, the distribution of the CIR model is not Gaussian, which makes it difficult to analyze.

The density function is given by:

$$f(X_s, s, X_t, t) = ce^{-(u+v)} \left(\frac{v}{u}\right)^{\frac{q}{2}} I_q(2\sqrt{uv})$$

where

$$\begin{aligned} c &= \frac{2\alpha}{\sigma^2(1 - e^{-\alpha\Delta t})} \\ u &= cX_s e^{-\alpha\Delta t} \\ v &= cX_t \\ q &= \frac{2\alpha\mu}{\sigma^2} - 1 \\ \Delta t &= t - s \end{aligned}$$

$I_q(\cdot)$ is a Bessel function of first type and order q :

$$I_q(x) = \sum_{j=0}^{\infty} \left(\frac{x}{2}\right)^{2j+q} \frac{1}{k!\Gamma(j+q+1)}$$

where Γ is the gamma function.

Let $z_t = 2cX_t$. Then the conditional distribution of z_t given z_s is an uncentered $\chi_d^2(2u)$, with $d = \frac{4\alpha\mu}{\sigma^2}$ degrees of freedom and the non-centrality parameter is $\lambda = 2u$.

Therefore

$$z_t|z_s \sim \chi^2(d, \lambda)$$

where:

$$d = \frac{4\alpha\mu}{\sigma^2}$$

$$\lambda = \frac{4\alpha}{\sigma^2(1 - e^{-\alpha\Delta t})} e^{-\alpha\Delta t} X_s$$

Since $z_t = 2cX_t$, X_t conditional on X_s has the same distribution as $z_t/2c$ conditional on $z_s/2c$. So,

$$X_t|X_s \sim \frac{z_t}{2c} | \frac{z_t}{2c} \sim \frac{1}{2c} \chi^2(d, \lambda)$$

We are going to make a study of the different behaviours that the deterministic solution of the CIR model equation can present in terms of the relations among the different parameters, which will be useful later to give an interpretation of the model parameters, although we know that the stochastic part would give oscillations with respect to said behaviour. We shall allow in this analysis for negative values of α since in certain regions of the data the calibrated values of α result in negative values. According to Eq. (7) we distinguish two cases, depending on whether X_t is greater or less than μ and in each case two subcases, depending on whether α is positive or negative:

1. If $X_t < \mu$:

- If $\alpha > 0$, X_t approaches μ from below.
- If $\alpha < 0$, X_t moves away from μ downwards.

2. If $X_t > \mu$:

- If $\alpha > 0$, X_t approaches μ from above.
- If $\alpha < 0$, X_t moves away from μ upwards.

1. Estimation of the parameters

To approximate the data well, it is necessary to give a good adjustment of the parameters. In the case of the CIR* model, we must estimate three parameters, α , μ and σ . We will generally refer to them as the parameter vector $\theta \equiv (\alpha, \mu, \sigma)$. The procedure that will be followed to estimate the parameters is the one shown in [30] and it is the maximum likelihood method (MLE), which is based on maximizing the objective function under consideration. For the maximum likelihood estimation of the parameter vector $\theta \equiv (\alpha, \mu, \sigma)$ the transition densities are required. The CIR process is one of the processes for which we know its density function explicitly. Given X_t at time t , the density of $X_{t+\Delta t}$ at time $t + \Delta t$ is:

$$p(X_{t+\Delta t}|X_t; \theta, \Delta t) = ce^{-(u+v)} \left(\frac{v}{u}\right)^{\frac{q}{2}} I_q(2\sqrt{uv})$$

where

$$\begin{aligned} c &= \frac{2\alpha}{\sigma^2(1 - e^{-\alpha\Delta t})} \\ u &= cX_t e^{-\alpha\Delta t} \\ v &= cX_{t+\Delta t} \\ q &= \frac{2\alpha\mu}{\sigma^2} - 1 \end{aligned}$$

where $I_q(2\sqrt{uv})$ is a Bessel function.

The likelihood function for time series with N observations is:

$$L(\theta) = \prod_{i=1}^{N-1} p(X_{t_{i+1}}|X_{t_i}; \theta, \Delta t) \quad (9)$$

To simplify the calculations, it is usual to work with the log-likelihood expression, which consists of taking logarithms in the equation (9).

$$\ln L(\theta) = \sum_{i=1}^{N-1} \ln p(X_{t_{i+1}}|X_{t_i}; \theta, \Delta t) \quad (10)$$

from which the log-likelihood function of the CIR process can be easily derived.

$$\ln L(\theta) = (N-1) \ln c + \sum_{i=1}^{N-1} \left[-u_{t_i} - v_{t_{i+1}} + \frac{1}{2}q \ln \left(\frac{v_{t_{i+1}}}{u_{t_i}} \right) + \ln \left(I_q \left(2\sqrt{u_{t_i} v_{t_{i+1}}} \right) \right) \right] \quad (11)$$

where $u_{t_i} = cX_{t_i} e^{-\alpha\Delta t}$ y $v_{t_{i+1}} = cX_{t_{i+1}}$

To find the maximum likelihood estimate $\hat{\theta}$ of the parameter vector θ , we have to maximize the function (11) over its parameter space.

$$\hat{\theta} = (\hat{\alpha}, \hat{\mu}, \hat{\sigma}) = \arg \max_{\theta} \ln L(\theta) \quad (12)$$

Since the logarithm function is monotonically increasing, maximizing the log-likelihood function is equivalent to maximizing the likelihood function.

To solve the problem (12) we resort to numerical computation. For the global optimal convergence, the initial optimization points are essential, for which the method of least squares will be used. We first write the equation of the discretized CIR*:

$$X_{t+\Delta t} - X_t = \alpha(\mu - X_t)\Delta t + \sigma\sqrt{X_t}W_t \quad (13)$$

where W_t is distributed with zero mean and variance Δt .

Dividing the equation (13) by $\sqrt{X_t}$ we get:

$$\frac{X_{t+\Delta t} - X_t}{\sqrt{X_t}} = \frac{\alpha\mu\Delta t}{\sqrt{X_t}} - \alpha\sqrt{X_t}\Delta t + \sigma W_t$$

Based on this expression, the initial values of $\hat{\alpha}$ and $\hat{\mu}$ are found by minimizing the function:

$$(\hat{\alpha}, \hat{\mu}) = \arg \min_{\alpha, \mu} \sum_{i=1}^{N-1} \left(\frac{X_{t_{i+1}} - X_{t_i}}{\sqrt{X_{t_i}}} - \frac{\alpha\mu\Delta t}{\sqrt{X_{t_i}}} + \alpha\sqrt{X_{t_i}}\Delta t \right)^2$$

The exact expression of the solution is found on page 3 of [30]. The estimate of $\hat{\sigma}$ is found as the standard deviation of the residuals.

To optimize the objective function (11) we need to evaluate the Bessel function $I_q(2\sqrt{uv})$. The function *besseli* is implemented in Matlab, but this usually causes problems, because the function $I_q = (2\sqrt{uv})$ approaches infinity very quickly. Fortunately, Matlab allows us to give another scaled version, which we will call $I_q^1(2\sqrt{uv})$, which solves the divergence problem in such a way that:

$$I_q^1(2\sqrt{uv}) = I_q(2\sqrt{uv}) \exp(-2\sqrt{uv})$$

And therefore:

$$I_q(2\sqrt{uv}) = \frac{I_q^1(2\sqrt{uv})}{\exp(-2\sqrt{uv})}$$

Rewriting the expression (11) we get:

$$\begin{aligned} \ln L(\theta) = (N-1) \ln c + \sum_{i=1}^{N-1} (-u_{t_i} - v_{t_{i+1}} + \frac{1}{2} \ln \left(\frac{v_{t_{i+1}}}{u_{t_i}} \right) + \\ + \ln (I_q^1(2\sqrt{u_{t_i}v_{t_{i+1}}})) + 2\sqrt{u_{t_i}v_{t_{i+1}}}) \end{aligned}$$

2. Numerical methods

To obtain an approximation of the exact solution of the equation we need to establish a numerical scheme. In our case, we will implement the Euler-Maruyama and Milstein numerical schemes, to see later if there are notable differences between them.

The Euler-Maruyama scheme or method is an extension of Euler's method for ordinary differential equations to stochastic differential equations. Let be an Itô process $\{X_t, 0 \leq t \leq T\}$ that is the solution of the following stochastic differential equation:

$$\begin{cases} dX_t = f(t, X_t)dt + g(t, X_t)dW_t \\ X_0 = x_0 \end{cases} \quad (14)$$

where $W(t)$ represents the Wiener process and suppose we want to solve this SDE in the time interval $[0, T]$.

The Euler-Maruyama approximation Y_i to the true solution of X is defined as follows:

- Divide the interval $[0, T]$ in N subinterval of size $\Delta t = T/N$ being $0 = t_0 < t_1 < \dots < t_N = T$.
- Set the initial condition $Y_0 = x_0$.
- Define recursively Y_i for $1 \leq i \leq N$

$$Y_{i+1} = Y_i + f(t_i, Y_i)\Delta t + g(t_i, Y_i)\Delta W_i \quad (15)$$

where $\Delta W_i = W_{t_{i+1}} - W_{t_i}$.

The variables ΔW_i are independent and identically distributed normal random variables, that is, $\Delta W_i \sim \sqrt{\Delta t}Z$ with $Z \sim N(0, 1)$.

The Milstein method [31] is used to increase the accuracy of the Euler-Maruyama method. This is achieved by introducing a term of order 2 by using the partial derivative with respect to x of $g(t, x)$.

Given an Itô process $\{X_t, 0 \leq t \leq T\}$ which is a solution of the stochastic differential equation (14) the approximation of the Milstein method Y_i to the true solution of X is given by:

- Divide the interval $[0, T]$ into subintervals of size $\Delta t = T/N$ with $0 = t_0 < t_1 < \dots < t_n = T$.
- Take as initial condition $Y_0 = x_0$.
- Recursively define Y_i for $1 \leq i \leq N$ by:

$$Y_{i+1} = Y_i + f(t_i, Y_i)\Delta t + g(t_i, Y_i)\Delta W_i + \frac{1}{2}g(t_i, Y_i)\frac{\partial g(t_i, Y_i)}{\partial x}[(\Delta W_i)^2 - \Delta t] \quad (16)$$

where $\Delta W_i = W_{t_{i+1}} - W_{t_i}$.

The variables ΔW_i are independent and identically distributed normal random variables, that is, $\Delta W_i \sim \sqrt{\Delta t}Z$ with $Z \sim N(0, 1)$. As we can see, the expression of the scheme is the same as that of Euler, except that the summand is added

$$\frac{1}{2}g(t_i, Y_i)\frac{\partial g(t_i, Y_i)}{\partial x}[(\Delta W_i)^2 - \Delta t]$$

Therefore, if $\frac{\partial g(t, x)}{\partial x}$ turns out to be 0 this method is equivalent to the Euler-Maruyama method. When a method satisfies $E(|Y_i - X(t_i)|) \leq K(\Delta t)^\gamma$ for some γ , that method is said to be a strong approximation of order γ . Applying this, the Euler-Maruyama method is a strong approximation of order $\gamma = 1/2$ while the Milstein method is a strong approximation of order $\gamma = 1$ if $f(t, X_t)$ and $g(t, X_t)$ are C^1 functions. The functions with which we are working in these models comply with this, so the order of convergence of the Milstein method will always be greater than that of Euler-Maruyama.

IV. RESULTS

Since we have daily data we set the time step $\Delta t = 1$. To compare both the Euler-Maruyama and the Milstein methods and see that they fit the real data we have well, we are going to choose a specific time. A window of 100 data will be taken from the first real data available and the following 500 days will be estimated. The prediction is made for the day following the last one of the windows, the window is moved one unit to the right and the process is repeated.

Figure 5 shows the three estimates that we want to compare, but as is logical, with that size they are not seen in detail. This is because the figure shows a first glance at the obtained estimates. Next, Figure 6 represents the real data (in grey), the ARMAX model estimates (in magenta) and the ones calculated with the CIR* model (blue curve). As in the previous section, the Euler-Maruyama and Milstein methods are very similar, so the differences between the depicted curves cannot be seen unless a larger zoom is made.

It can be seen that the blue curve generally fits the real data better, so it stands to reason that the CIR* model is slightly better than the ARMAX model. To verify this rigorously, the root mean square error (RMSE) of the CIR* model has been calculated with the Euler-Maruyama and Milstein method, and the RMSE of the ARMAX model. These errors are collected in the following Table I. As we can see, the CIR* model gives better results than the ARMAX model.

	CIR* with Euler	CIR* with Milstein	ARMAX
RMSE	1.0556	1.0558	2.2157

TABLE I. Comparison of CIR* model errors (Euler-Maruyama and Milstein) and ARMAX

Finally, we are going to give an interpretation of the parameters of the CIR* model at different stages of the pandemic, based on the analysis of the deterministic solution of the CIR* model given just before Sec. III C 1.

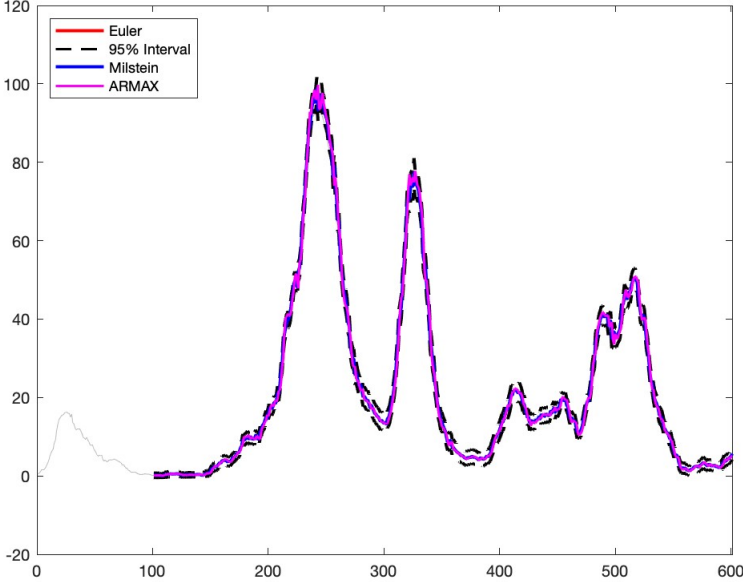


FIG. 5. Approximations of the CIR* with Euler-Maruyama and Milstein, and ARMAX with win=100, tin=1 and nsim=1000.

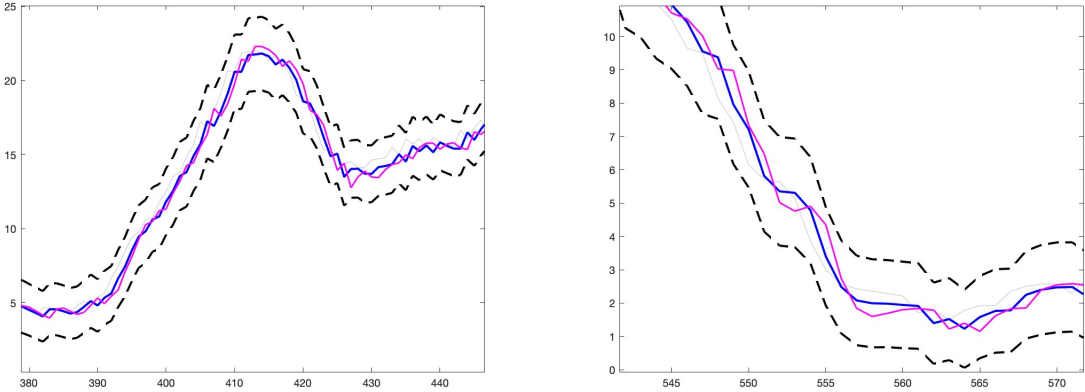


FIG. 6. Comparison of CIR* (blue) and ARMAX models (magenta)

We begin by studying a stage in which infections are increasing. For the estimated parameters to have the same trend, the window from which they are estimated must also be in the growth range, which will force us to take a small window and estimate few values, since if we look at Figure 1, we see that the periods in which the infections grow are not many days. Taking this into account, we are going to focus on the section that goes from day 210 to 229, that is, 20 forecasts, taking a window of 30 days. Based on the results obtained, we observe that both the mean of α and μ are negative. Since the estimated data values are greater than the mean, then X_t would move away from the mean upwards.

To corroborate that this is true, another stage of increase in cases of the pandemic has been taken, specifically from day 310 to 319, that is, 10 days, and a window of 30 days. The number of forecasts had to be reduced because, as previously mentioned, the window of days must be in the growth range for good analysis. In Figure 7 one can see both sections and in Table II, the exact values of the mean of the parameters in the two stages.

Keeping the ideas we used from the previous case, we now take a time in which the cases decrease. We estimate the time step that goes from day 265 to 284. In this case, we again obtain the negative mean of α , which makes sense, since in periods of strong growth or decrease the values move away from the mean. On the contrary, now the mean

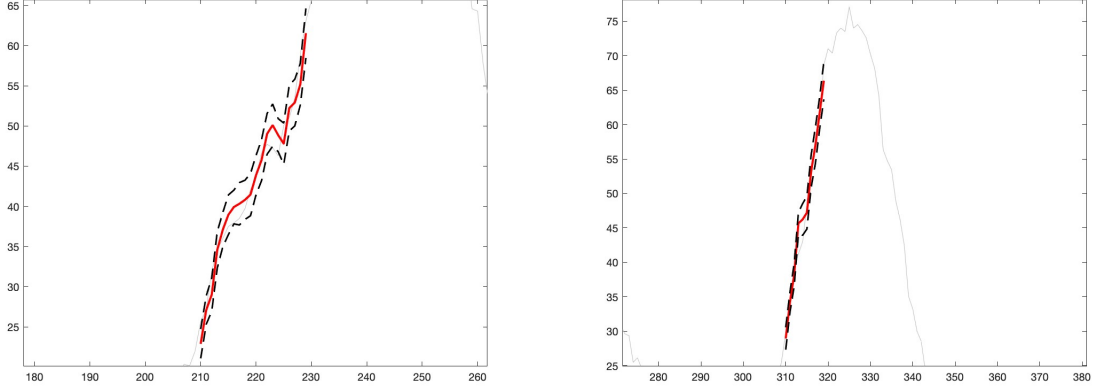


FIG. 7. Stage 1 (left) and stage 2 (right) of a steep growth of the COVID-19 pandemic daily cases.

	Stage 1	Stage 2
Average α	-0.0562	-0.0990
Average μ	-3.6346	-3.5105
Average σ	0.2253	0.2007

TABLE II. Growing stages of COVID-19 infections

of the parameter μ is very large and exceeds the mean of infections in that section, therefore, the values X are far from the mean, but this time below.

As in the previous case, another section has been taken to verify the results. The estimates of both stages can be seen in Figure 8 and the comparison of the mean values of the parameters in Table III.

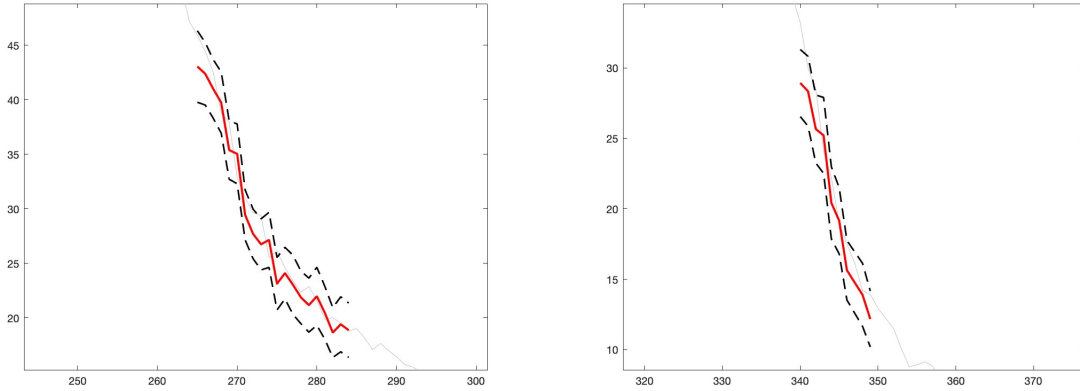


FIG. 8. Stage 3 (left) and stage 4 (right) of a decisive decrease in the daily cases of the COVID-19 pandemic.

	Stage 3	Stage 4
Average α	-0.01664	-0.0305
Average μ	190.5401	95.5082
Average σ	0.2644	0.2925

TABLE III. Decreasing of COVID-19 infections

Finally, we are going to interpret the parameters in a section where the values are relatively constant.

As seen in figure 1, there are a few sections where this occurs. We are going to take days between 110 and 139, in which it is observed that the COVID cases are close to the 0 value. This may seem surprising, but it makes sense because it precisely coincides with the state of alarm. As can be seen on the right side of the graph, from day 150 the cases begin to increase, coinciding with the de-escalation process and the summer of 2020 when restrictions were relaxed.

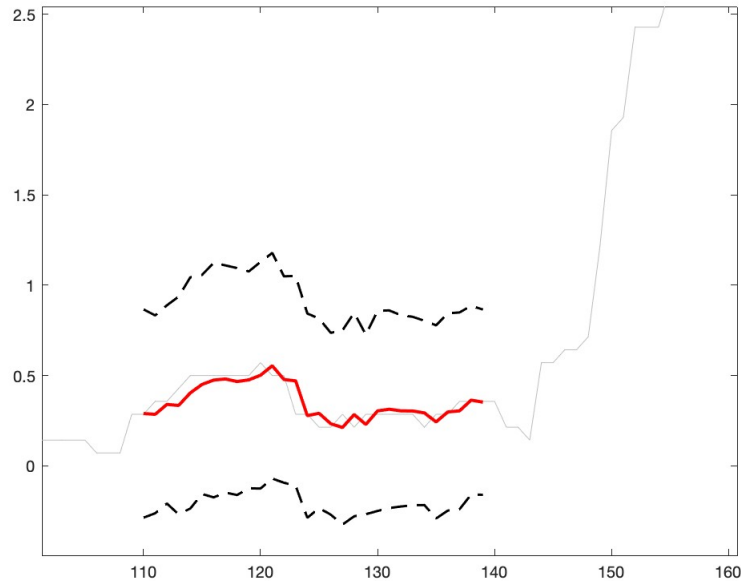


FIG. 9. Example of a stage of the COVID-19 pandemic where the number of cases are relatively flat.

At this stage, the mean of the parameters α is 0.1397, that is, positive, unlike the previous cases. The mean of the parameters μ is 0.3303 and that of σ is 0.1448, so we have a small deviation.

	Stage 5
Average α	0.1397
Average μ	0.3303
Average σ	0.1448

TABLE IV. Relatively constant stage of COVID-19 infections.

According to the analysis of the deterministic solution, X_t will oscillate around the mean, which makes sense, since the real mean of those days is around 0.33 and the value of the data varies between 0.25 and 0.55 cases.

V. CONCLUSIONS

The main objective of this work is the study and development of some stochastic models typically used in financial markets applied to the COVID-19 pandemic in the city of Jaén.

For solving stochastic equations both the Euler-Maruyama method and the Milstein method were used with reference to the CIR* stochastic process. Over the reported COVID-19 daily cases of the pandemic in the city of Jaén (Spain), the maximum likelihood method was used for parameters calibration. The forecasts given with this model have been validated with 95% confidence intervals and with statistical measures of goodness of fit, such as the RMSE (root mean square error). The results obtained are consistent with the observations and quite accurate. For comparison, the classical ARIMAX model has been used, resulting in more accurate predictions for the suggested CIR* model. The reason could be the relatively small size of the city of Jaén, causing large fluctuations in the number of cases that are not sufficiently softened by the moving averages, resulting in a worse behaviour of ARIMAX in comparison with CIR*. The importance of the suggested approach is twofold because it not only extends the models available to

scholars to model pandemics, but also paves the way for similar approaches in which financial models can be converted into econometric models.

Future research could be aimed at enlarging the scope to all provinces of Andalusia. In such a case, we could expect that a greater number of data could imply a longer time for the trend to change. In addition, the number of healed and deceased could also be studied, although the latter, being much smaller, will present the aforementioned problems. In terms of considered models, future research could include a comparison with the more advanced CIR# by Orlando et al. [19, 24–26]. In addition, although our work has only been done for one equation, it could also be generalized to systems of equations to discover the interrelation between different cities. Finally, note that stochastic differential equations are not only a very powerful tool for modelling economic-financial variables, but also in the epidemiological field, being proven from this practical point of view.

ACKNOWLEDGMENTS

G.O. is a member of the research group of GNAMPA - INdAM (Italy). J.G. acknowledges Spanish MICINN through the project PGC2018-097831-B-I00 and Junta de Andalucía through the project FEDER-UJA-1381026.

CONFLICT OF INTEREST

The authors declare there is no conflict of interest.

-
- [1] Mills TC, Mills TC. Time Series Techniques for Economists. Cambridge, England, UK: Cambridge University Press; 1990. Available from: https://books.google.es/books/about/Time_Series_Techniques_for_Economists.html?id=cNe3xrFg3PcC&redir_esc=y.
 - [2] Lee MH, Hamzah N, et al. Calendar variation model based on ARIMAX for forecasting sales data with Ramadhan effect. In: Proceedings of the Regional Conference on Statistical Sciences. vol. 10; 2010. p. 30-41.
 - [3] Chadsuthi S, Modchang C, Lenbury Y, Iamsirithaworn S, Triampo W. Modeling seasonal leptospirosis transmission and its association with rainfall and temperature in Thailand using time-series and ARIMAX analyses. Asian Pacific Journal of Tropical Medicine. 2012 Jul;5(7):539-46.
 - [4] Suharsono A, Suhartono, Masyitha A, Anuravega A. Time series regression and ARIMAX for forecasting currency flow at Bank Indonesia in Sulawesi region. AIP Conf Proc. 2015 Dec;1691(1):050025.
 - [5] Anggraeni W, Vinarti RA, Kurniawati YD. Performance Comparisons between Arima and Arimax Method in Moslem Kids Clothes Demand Forecasting: Case Study. Procedia Comput Sci. 2015 Jan;72:630-7.
 - [6] Shilpa G, Sheshadri G. ARIMAX model for short-term electrical load forecasting. Int J Recent Technol Eng(IJRTE). 2019;8(4).
 - [7] Ariyo AA, Adewumi AO, Ayo CK. Stock Price Prediction Using the ARIMA Model. In: 2014 UKSim-AMSS 16th International Conference on Computer Modelling and Simulation. IEEE; 2014. p. 106-12.
 - [8] Subramaniam G, Muthukumar I. Efficacy of time series forecasting (ARIMA) in post-COVID econometric analysis. undefined. 2020. Available from: [https://www.semanticscholar.org/paper/Efficacy-of-time-series-forecasting-\(ARIMA\)-in-Subramaniam-Muthukumar/e6f06efef83b26b52dea243877bb925f45de05a4](https://www.semanticscholar.org/paper/Efficacy-of-time-series-forecasting-(ARIMA)-in-Subramaniam-Muthukumar/e6f06efef83b26b52dea243877bb925f45de05a4).
 - [9] Orlando G, Bufalo M. Modelling bursts and chaos regularization in credit risk with a deterministic nonlinear model. Finance Research Letters. 2022 Jun;47:102599.
 - [10] Orlando G, Bufalo M, Stoop R. Financial markets' deterministic aspects modeled by a low-dimensional equation. Sci Rep. 2022 Feb;12(1693):1-13.
 - [11] Ekinci A. Modelling and forecasting of growth rate of new COVID-19 cases in top nine affected countries: Considering conditional variance and asymmetric effect. Chaos, Solitons Fractals. 2021 Oct;151:111227.
 - [12] Sahai AK, Rath N, Sood V, Singh MP. ARIMA modelling & forecasting of COVID-19 in top five affected countries. Diabetes & Metabolic Syndrome: Clinical Research & Reviews. 2020 Sep;14(5):1419-27.
 - [13] Katoch R, Sidhu A. An Application of ARIMA Model to Forecast the Dynamics of COVID-19 Epidemic in India. Global Business Review. 2021 Mar:0972150920988653.
 - [14] Suhartono, Lee MH, Prastyo DD. Two levels ARIMAX and regression models for forecasting time series data with calendar variation effects. AIP Conf Proc. 2015 Dec;1691(1):050026.
 - [15] Tanyavutti A, Tanlamai U. ARIMAX versus Holt Winter methods: the case of blood demand prediction in Thailand. International Journal of Environmental & Science Education. 2018;13(6):519-25.
 - [16] Cox JC, Ingersoll JE, Jr, Ross SA. A Theory of the Term Structure of Interest Rates. Econometrica. 1985 Mar;53(2):385-407. Available from: <https://www.jstor.org/stable/1911242?origin=crossref>.

- [17] Cox JC, Ingersoll JE, Jr, Ross SA. A Theory of the Term Structure of Interest Rates. In: Theory of Valuation. Singapore: WORLD SCIENTIFIC; 2005. p. 129-64.
- [18] Vasicek O. An equilibrium characterization of the term structure. *Journal of Financial Economics*. 1977 Nov;5(2):177-88.
- [19] Orlando G, Mininni RM, Bufalo M. A new approach to CIR short-term rates modelling. In: *New Methods in Fixed Income Modeling*. Springer; 2018. p. 35-43.
- [20] Canale A, Mininni RM, Rhandi A. Analytic approach to solve a degenerate parabolic PDE for the Heston model. *Mathematical Methods in the Applied Sciences*. 2017;40(13):4982-92.
- [21] Orlando G, Tagliatela G. A review on implied volatility calculation. *Journal of Computational and Applied Mathematics*. 2017;320:202-20.
- [22] Duffie D. Credit risk modeling with affine processes. *Journal of Banking & Finance*. 2005;29(11):2751-802.
- [23] Orlando G, Bufalo M, Penikas H, Zurlo C. *Modern Financial Engineering | Topics in Systems Engineering*. vol. 2. Singapore: World Scientific Publishing Company; 2021.
- [24] Orlando G, Mininni RM, Bufalo M. Interest rates calibration with a CIR model. *Journal of Risk Finance*. 2019 Sep;20(4):370-87.
- [25] Orlando G, Mininni RM, Bufalo M. Forecasting interest rates through Vasicek and CIR models: A partitioning approach. *Journal of Forecasting*. 2020;39(4):569-79.
- [26] Orlando G, Bufalo M. Interest rates forecasting: Between Hull and White and the CIR#—How to make a single-factor model work. *Journal of Forecasting*. 2021 Dec;40(8):1566-80.
- [27] Ljung L. System Identification. In: *Signal Analysis and Prediction*. Boston, MA, USA: Birkhäuser, Boston, MA; 1998. p. 163-73.
- [28] MathWorks. Estimate ARMAX Model Example; 2022. [Online; accessed 18. Nov. 2022]. Available from: <https://www.mathworks.com/help/ident/ref/armax.html>.
- [29] Stoica P, Selen Y. Model-order selection: a review of information criterion rules. *IEEE Signal Process Mag*. 2004 Jul;21(4):36-47.
- [30] Kladičko K. Maximum likelihood estimation of the Cox-Ingersoll-Ross process: the MATLAB implementation. *Technical Computing Prague*. 2007;7(8).
- [31] Milstein GN. Approximate integration of stochastic differential equations. *Theory of Probability & its Applications*. 1975;19(3):557-62.